

Converting AC Distribution Lines to DC to Increase Transfer Capacities and DG Penetration

Lu Zhang¹, Member, IEEE, Jun Liang, Senior Member, IEEE, Wei Tang, Member, IEEE, Gen Li, Yongxiang Cai², and Wanxing Sheng, Senior Member, IEEE

Abstract—Transfer capacities of urban distribution networks need to be increased to fulfill the increasing load demands and to accommodate distributed generation (DG). However, there are limited spaces to build new substations and lines, and curtailment of DGs may happen due to voltage violation during DG outputs fluctuation. This paper proposes and analyzes various methods to convert some existing ac MV lines to dc lines in order to form a hybrid ac/dc distribution network, based on which transfer capacities of lines can be increased, and flexible power shift can be achieved through a voltage source converter between two lines. The increases of transfer capacities are quantified. Optimal operation to fully utilize the increased capacities is achieved, in which losses are minimized in day-ahead scheduling, and node voltages are regulated real-time within security ranges based on limited measurement. Not only reactive power but also real power optimization are designed to maximize load supply and DG accommodation. A sensitivity method is proposed considering relatively large r/x ratio of an MV distribution network, which is effective for the real-time voltage regulation. Simulations are performed to verify the proposed method.

Index Terms—Hybrid AC/DC, distribution network, converting AC to DC, transfer capacity, DG accommodation.

I. INTRODUCTION

IN URBAN areas, transfer capabilities of existing AC distribution lines need to be increased to meet the increasing load demands and the requirements of high reliability and

power quality. However, existing AC distribution lines are facing challenges of managing load demand growth in urban areas [1]. Moreover, the costs of distribution line corridors become higher in urban areas. There are very limited spaces to build new substations and distribution lines.

On the other hand, with the integration of large scale, dispersed renewable sources, distribution networks face a challenge of voltage control due to the intermittence of distributed generation (DG) [2]. Curtailment of wind power and photovoltaic (PV) may take place, because power flow cannot be flexibly scheduled in a traditional distribution network. Therefore, improving transfer capacity and accommodating DG are two main serious issues at present.

Distribution lines in urban areas are normally close to each other. Due to load fluctuation, power in a distribution line keeps changing. For two adjacent lines, if one line is lightly loaded while the other is heavily loaded, power losses and voltage deviations will be high in a heavy loaded line. Loads may have to be shed to avoid over loading. Meanwhile, DG curtailment will happen in light loaded lines in order to alleviate over-voltage problems. Flexible power shift between two adjacent distribution lines might be a way to meet the operation requirement of variable power injection of DG and loads fluctuation so as to increase overall power transfer capacity. However, AC distribution lines are normally operated as a radial network, because closed-loop operation in AC distribution networks will cause circulating currents due to different phase angles or amplitudes.

Reconfiguration has been widely used in distribution networks [3] to achieve load transfer between two feeders. However, a large transient current will be generated when closing the loop. This could mis-trip AC circuit breakers due to over-current protection, and lead to service interruption [4]. Moreover, closed loop structures might produce circulation of zero-sequence current because of unbalanced serial impedance in lines [5]. Operation costs will be increased due to frequent switching because of wear and tear on circuit breakers [3]. Therefore, it is very difficult to achieve real-time optimal power transfer through network reconfiguration.

Power electronic devices have been used in AC distribution networks [1], [6], [7]. Reference [1] proposed to utilize dc-links to merge heavily-meshed urban distribution networks to increase reliability and expand operational flexibility. Reference [6] provided a comparison of power electronic devices which can be used in distribution networks in order to accommodate large amounts of DGs. Reference [7] proposed

Manuscript received December 7, 2016; revised March 29, 2017; July 3, 2017, and September 22, 2017; accepted October 19, 2017. Date of publication January 1, 2018; date of current version February 18, 2019. This work was supported in part by the National Natural Science Foundation of China under Grant 51377162, and in part by the National Key Research and Development Program of China under Grant 2017YFB0903000. The work of J. Liang was supported by EPSRC Project under Grant EP/L021455/1. The work of G. Li was supported by the People Programme (Marie Curie Actions) of the European Union's Seventh Framework Programme under Grant FP7/2007-2013 under REA Project Title MEDOW under Agreement 317221. Paper no. TSG-01717-2016. (Corresponding author: Wei Tang.)

L. Zhang, W. Tang, and Y. Cai are with the College of Information and Electrical Engineering, China Agricultural University, Beijing 100083, China (e-mail: luzhang0210@gmail.com; wei_tang@cau.edu.cn; lpscaiyx@163.com).

J. Liang and G. Li are with the School of Engineering, Cardiff University, Cardiff CF24 3AA, U.K. (e-mail: liangj1@cardiff.ac.uk; lig9@cardiff.ac.uk).

W. Sheng is with the Power Distribution Department, China Electric Power Research Institute, Beijing 100192, China (e-mail: wxsheng@epri.sgcc.com.cn).

Color versions of one or more of the figures in this paper are available online at <http://ieeexplore.ieee.org>.

Digital Object Identifier 10.1109/TSG.2017.2768392

to use back-to-back converters to connect AC lines for reducing power losses and improve node voltages. However, the DC side of these power electronic devices is not utilized for power transfer or DG integration. The maximum transfer power capacity of each AC line is not increased.

Therefore, distribution networks are facing challenges with the increasing load demand and DG accommodation, large variation of DG power outputs, large transient impact of the conventional power rescheduling, and limited transfer capacity of existing circuits. Cost-effective solutions must be sought to increase the power transfer capacity without constructing new lines, to reschedule power between lines flexibly and to control real and reactive power independently. A hybrid AC/DC distribution network, which can be formed through converting some of existing AC lines to DC, can meet these requirements, particularly in places with very limited way-leave such as urban areas.

Hybrid AC/DC technologies have been used for high voltage transmission [8], [9], distribution networks [10]–[12] and low voltage microgrids [13], [14]. Conversion of existing AC lines to DC operation has been presented in CIGRE report [15], and proposed in various voltage levels [16], [17] as an innovative method to increase power capability of existing lines.

One of the drawbacks for converting AC lines to DC operation is the cost of building voltage source converters (VSCs) for connecting AC lines and AC loads. However these costs would be much lower than the cost reduction by deferring or removing the need of constructing new AC lines [1], [18]. Another drawback is the operation power losses of the VSCs, which are needed to convert AC lines to DC operation. However, the flexible power dispatch of VSCs can reduce AC and DC line losses. This trade-off, particularly possible overall power loss reduction, is worth of investigation. In addition, there are some other technical drawbacks for converting AC lines to DC operation, which include Electro Magnetic Interference (EMI), DC stress (polarization) of materials designed for AC [15], DC creepage on insulators, corrosion of structures on the path of return current if a return conductor is not used [16], [17], and other environment impacts [19], which are out of scope of this paper, and can be studied in the future.

This paper analyzes and quantifies the capacity increases of various methods to convert AC lines to DC ones suitable for urban areas. Contributions include the methods to fully utilize the increased line capacity, in which losses are minimized in day-ahead scheduling, and node voltages are regulated within security ranges real-time in case of forecast errors. Not only reactive power but also real power optimization are designed to maximize load supply and DG accommodation, based on limited measurement of node voltages.

The effect of power variation on node voltages is normally analyzed using a sensitivity method [20], [21]. However these methods can only be used in radial networks due to their limits of power flow equations. The inverse Jacobian matrix of Newton Raphson algorithm [22] can be used for mesh configurations but suffers convergence problem for networks with high r/x ratio. This paper proposes a sensitivity

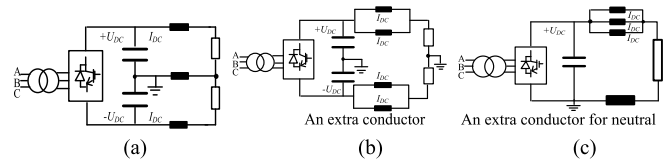


Fig. 1. DC link configurations converted from AC lines (a) Symmetrical configuration with a neutral wire (b) Symmetrical configuration without neutral wire (c) Asymmetrical configuration with a neutral wire.

method considering high r/x ratio and closed-loop topologies for hybrid AC/DC MV distribution networks, which is effective for the real-time voltage regulation. The sensitivities of AC and DC lines in this paper are decoupled by VSC because of its independent control ability of active and reactive power.

II. HYBRID AC/DC DISTRIBUTION NETWORKS

A. DC Links Converted From AC Distribution Lines

When converting an AC line to DC, if a symmetrical configuration is chosen for the VSC station, the three AC wires are used as a positive DC wire, a negative DC wire and a neutral wire respectively, as shown in Fig. 1(a). The neutral wire provides a return path for unbalanced DC currents. This configuration has low utilization of the wires, but can avoid ground return of unbalanced load currents, because only two of the three wires are used for power transfer, and the other one is only used for neutral.

If a symmetrical configuration without neutral wire is chosen, one extra conductor which has the same rating can be added in order to make full use of the third existing wire and further increase transfer capacities. Therefore, both the positive and negative poles are formed using two wires as shown in Fig. 1(b). Utilization of wires is increased using this configuration but a ground return is used for unbalanced load current, which has potential safety risks.

If an asymmetrical configuration is chosen for the VSC, the three wires are combined as one DC wire, but an extra conductor is needed as a neutral wire, which is grounded, as shown in Fig. 1(c). The neutral wire is fully rated for the load current but only lightly insulated with nearly zero volt potential, thereby reducing the costs.

In urban distribution networks, three-core underground cables and double circuit lines are widely used due to limited corridor spaces. There are various methods to convert urban distribution AC lines to DC as illustrated in Table I. The maximum power transfer capacity for each case is also given.

The maximum DC voltage can be larger than the peak value of an AC voltage as a Cigre technical brochure [23] suggests that on the basis of electric mean stress the cable insulation could withstand roughly twice the RMS AC voltage as an applied DC voltage, and 1.5 times taking into account ageing factors. Corona effects with DC voltage may be less severe than with AC, and internal over voltages in DC systems have a lower ratio than AC switching over voltages. The AC peak voltage, i.e., 1.414 times the RMS AC voltage, has been

proposed as a conservative operating voltage in a practical MVDC project [24]. On the other hand, insulator pollution may be an obstacle to a high DC voltage level since insulator pollution is more crucial under DC voltage. Besides, DC voltage is also constrained by acceptable levels of audible noise in dry weather as well as electric field and space charge current at ground level [15]. Long term degradation, polarization and aging of the insulation material are subject to further monitoring. Therefore, considering above effects, this paper selects the maximum DC voltage to be the peak value of the AC voltages, either line-ground voltages or line-line voltages depending on configurations.

When converting a 3-core AC cable to DC operation, as for the cases in Fig. 1(a) and (b), the total DC voltage is $2U_{DC} = \sqrt{2}U_{AC}$. Since both the positive and negative poles are within the same cable, the maximum voltage is determined by the insulation to withstand the peak line-line voltage. Thus

$$U_{DC} = \sqrt{2}/2 U_{AC} \quad (1)$$

For the case in Fig. 1 (c), the DC voltage is

$$U_{DC} = \sqrt{2}/\sqrt{3} U_{AC} \quad (2)$$

as the 3 cores have the same voltage, the maximum voltage is determined by the insulation for core-to-ground voltage. This also applies to the symmetrical without neutral configuration for double circuit cables, and all overhead line cases.

The resistances of DC lines are smaller than those of AC lines due to skin effect and proximity effect, which can be given by the equation (3) [25]:

$$r_{AC} = r_{DC} \cdot (1 + y_s + y_p) \quad (3)$$

where y_s is the skin effect factor; y_p is the proximity effect factor. y_s is about 0.02 for a typical Copper 7 STRD 0.328 Inches cable [26] under a working temperature of 40 °C and y_p is about 0.001 [19], [27]. Therefore the DC resistance is

$$r_{DC} = 0.98r_{AC} \quad (4)$$



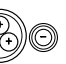

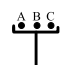
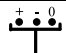
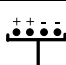
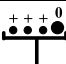
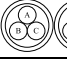

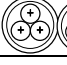
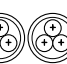

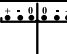

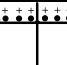
Considering the heat dissipation capability of a conductor for both AC and DC operation is the same, $I_{DC}^2 r_{DC} = I_{AC}^2 r_{AC}$, the maximum allowed DC current is thus obtained as

$$I_{DC} = 1.01I_{AC} \quad (5)$$

Moreover, an AC line carries more or less reactive power, a typical power factor $\cos\phi = 0.9$ of a MV line under normal operation is used.

The maximum transfer capacities of AC or DC circuits P_{\max} are given in Table I. The ratio of P_{\max} of each circuit to that of the AC circuit $P_{\max-AC}$ is $\sigma = \frac{P_{\max}}{P_{\max-AC}}$. For example, for the symmetrical configuration with a neutral wire in Fig. 1(a), $P_{\max} = 2U_{DC}I_{DC} = 1.428U_{AC}I_{AC}$ by using equations (1)-(3) and (5), and $\sigma = \frac{P_{\max}}{P_{\max-AC}} = \frac{1.428U_{AC}I_{AC}}{\sqrt{3}U_{AC}I_{AC}\cos\phi} = 0.916$. Table I has summarized the ratios for various cases.

TABLE I
CONVERSION METHODS

(a) Single circuit three-core underground cable			
Configuration		P_{\max}	σ
3-phase AC 		$\sqrt{3}U_{AC} \cdot I_{AC} \cos\phi$	1
DC	Symmetrical with neutral wire 	$2U_{DC}I_{DC}$	0.916
	Symmetrical without neutral wire with an extra conductor 	$4U_{DC}I_{DC}$	1.832
	Asymmetrical with an extra conductor as neutral wire 	$3U_{DC}I_{DC}$	1.587
(b) Single circuit overhead line			
Configuration		P_{\max}	σ
3-phase AC 		$\sqrt{3}U_{AC} \cdot I_{AC} \cos\phi$	1
DC	Symmetrical with neutral wire 	$2U_{DC}I_{DC}$	1.058
	Symmetrical without neutral wire with an extra conductor 	$4U_{DC}I_{DC}$	2.116
	Asymmetrical with an extra conductor as neutral wire 	$3U_{DC}I_{DC}$	1.587
(c) Double circuit three-core underground cable			
Configuration		P_{\max}	σ
3-phase AC 		$2\sqrt{3}U_{AC} \cdot I_{AC} \cos\phi$	1
DC	Symmetrical with neutral wire 	$4U_{DC}I_{DC}$	0.916
	Symmetrical without neutral wire 	$6U_{DC}I_{DC}$	1.587
	Asymmetrical with an extra conductor as neutral wire 	$6U_{DC}I_{DC}$	1.587
(d) Double circuit overhead line			
Configuration		P_{\max}	σ
3-phase AC 		$2\sqrt{3}U_{AC} \cdot I_{AC} \cos\phi$	1
DC	Symmetrical with neutral wire 	$4U_{DC}I_{DC}$	1.058
	Symmetrical without neutral wire 	$6U_{DC}I_{DC}$	1.587
	Asymmetrical using ground return 	$6U_{DC}I_{DC}$	1.587

B. Network Losses

The maximum allowed power losses of a line for AC or DC operation are the same due to the heat dissipation capability of a conductor. Thus losses are compared under a same transfer

power. For given real and reactive power P_l and Q_l of an AC line, the power loss is:

$$P_{loss}^{AC} = \frac{P_l^2 + Q_l^2}{U_{AC}^2} r_{AC} \quad (6)$$

For the case in Fig. 1(a), power loss in a DC line carrying the same power P_l is:

$$P_{loss}^{DC} = \frac{P_l^2}{2U_{DC}^2} \cdot r_{DC} \quad (7)$$

For the case in Fig. 1(b), power loss in a DC line carrying the same power P_l is:

$$P_{loss}^{DC} = \frac{P_l^2}{4U_{DC}^2} \cdot r_{DC} \quad (8)$$

For the case in Fig. 1(c), power loss in a DC line carrying the same power P_l is:

$$P_{loss}^{DC} = \frac{2P_l^2}{3U_{DC}^2} \cdot r_{DC} \quad (9)$$

as there is no reactive power in a DC line, full current rating can be used to transfer real power.

Thus by using (1-9) and considering a typical power factor 0.9 of an AC line, the ratio of the losses between P_{loss}^{DC} and P_{loss}^{AC} are 0.794, 0.397 and 0.794 for cases in Fig. 1(a), (b) and (c), respectively.

C. Voltage Drop

An AC voltage drop under P_l can be calculated as:

$$\Delta U_{AC} = \frac{P_l \cdot r_{AC} + Q_l \cdot x_{AC}}{U_{AC}} \quad (10)$$

For the case in Fig. 1(a), a DC voltage drop can be calculated as:

$$\Delta U_{DC} = \frac{P_l}{2 \cdot U_{DC}} \cdot r_{DC} \quad (11)$$

For the case in Fig. 1(b), a DC voltage drop can be calculated as:

$$\Delta U_{DC} = \frac{P_l}{4 \cdot U_{DC}} \cdot r_{DC} \quad (12)$$

For the case in Fig. 1(c), a DC voltage drop can be calculated as:

$$\Delta U_{DC} = \frac{P_l}{3U_{DC}} \cdot r_{DC} \quad (13)$$

Thus by using (1)-(5), (10)-(13) and considering a typical power factor of 0.9 and a r_{AC}/x_{AC} ratio of 1.7 that is within a reasonable range between 1 and 2 [28] of an AC line, the ratios of voltage drops of a DC line to an AC line, $\Delta U_{DC}/\Delta U_{AC}$, are 0.539, 0.27, and 0.311 respectively for the three cases.

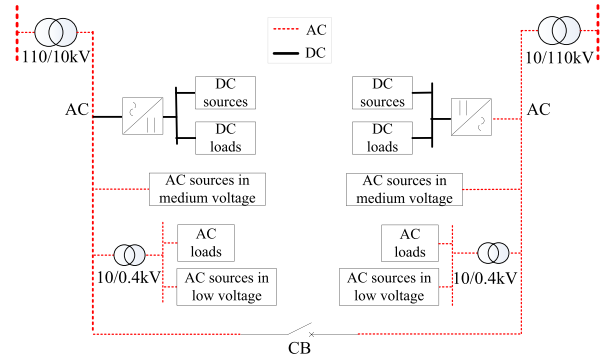


Fig. 2. A traditional structure of MV distribution network.

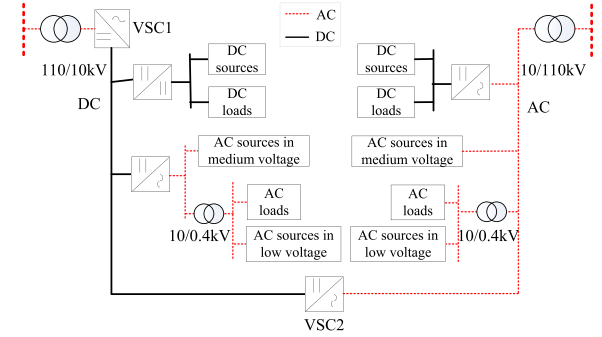


Fig. 3. A hybrid AC/DC distribution network.

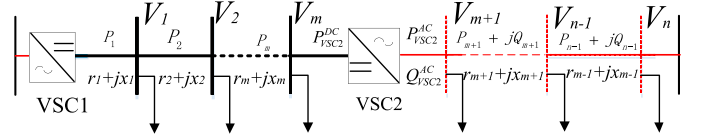


Fig. 4. Model of a hybrid AC/DC distribution network.

III. OPTIMIZATION FOR HYBRID AC/DC DISTRIBUTION NETWORK OPERATION

A. Structure of MV Distribution Networks

A typical MV AC distribution network is shown in Fig. 2. Two feeders from different substations are interconnected through a circuit-breaker (CB), which is normally opened. Due to the increase of load demand and DG, the AC lines are becoming overloaded. In order to deal with this issue, one AC line is converted to DC operation. Fig. 3 shows a hybrid AC/DC distribution network structure, in which an AC line is converted to DC and supplied through a VSC (VSC1), and the CB is replaced by a VSC (VSC2) to interconnect the AC and DC lines.

B. Optimization Strategy

A generic model of the two-feeder hybrid AC/DC network is given in Fig. 4 with m DC nodes and $(n-m)$ AC nodes. VSC1 controls the DC voltage and VSC2 controls real and reactive power to the AC line.

Through flexible control of VSC2, it is possible to achieve optimal power scheduling between the AC and DC lines to reduce overall power losses and regulate AC voltages.

Optimization has been designed for VSC2, which includes two modes, loss reduction mode and voltage regulation mode.

1) *Loss Reduction Mode*: The primary optimization objective is to minimize system losses when VSC2 operates in the loss reduction mode. The optimization variables are loads of all nodes, DG outputs, and power of VSC2. Optimization outputs are the real and reactive power of VSC2 for each hour of next day.

$$\min_{P_{VSC2}^{AC}, Q_{VSC2}^{AC}} P_{loss}(P_{load}, Q_{load}, P_{DG}, Q_{DG}, P_{VSC2}^{AC}, Q_{VSC2}^{AC}) \quad (14)$$

$$P_{loss} = P_{loss}^{DC} + P_{loss}^{AC} + P_{loss}^{VSC} \quad (15)$$

where P_{loss} is the total power losses of the hybrid AC/DC distribution network; P_{loss}^{DC} and P_{loss}^{AC} are losses in DC lines and AC lines. P_{loss}^{VSC} is the total losses of VSC1, VSC2 and VSCs for connecting AC loads to the DC lines, which can be calculated through a following equation [29], and has been used in distribution networks [30],

$$P_{loss}^{VSC} = aI_{VSC}^2 + bI_{VSC} + c \quad (16)$$

where I_{VSC} is the AC current of the VSC; a and b are the factors representing quadratic and linear dependency of converter losses on the converter current; c indicates no-load converter losses.

Constraint conditions for the optimization are

$$\begin{cases} P_l^{DC} \leq P_{max}^{DC} & l \in [1, m] \\ S_l^{AC} \leq S_{max}^{AC} & l \in [m+1, n] \\ \sqrt{P_{VSC2}^{AC2} + Q_{VSC2}^{AC2}} \leq S_{max}^{VSC} \\ V_{min} \leq V_i \leq V_{max} \end{cases} \quad (17)$$

where P_l^{DC} is the power of DC line l , P_{max}^{DC} is the DC line capacity; S_l^{AC} is the power of AC line l ; S_{max}^{AC} is the AC line capacity; S_{max}^{VSC} is power rating of the VSC; V_i is the voltage at node i , V_{min} and V_{max} are the minimum and maximum limits of the voltage security range, which are 0.95 p.u and 1.05 p.u.

A day-ahead optimization based on forecasted loads and DGs is performed only once every day, in order to obtain optimal hourly active and reactive power P_{VSC2}^{AC} and Q_{VSC2}^{AC} of VSC2 for next 24 hours.

The optimization was solved through Genetic Algorithm, and the optimization outputs (P_{VSC2}^{AC} , Q_{VSC2}^{AC}) were fed for AC-DC power flow [31] to calculate power losses which are further used for next optimization procedure. This iteration will be performed until optimal results are obtained.

2) *Voltage Regulation Mode*: However, voltage violations may occur because of forecast errors of DGs and loads. A real-time voltage regulation mode is developed to ensure node voltages within the security range. A voltage-sensitivity approach [21] is used to regulate the voltage efficiently through VSC2 control based on voltages measured at certain nodes. It should be noted that as only limited node voltages can be measured and available for VSC2 during operation, global optimization cannot be achieved at this stage without knowing other voltage and load/DG power.

The voltage regulation mode is triggered if a node voltage is above 1.05 p.u or below 0.95 p.u. VSC2 will switch back

to the loss reduction mode originally determined by the day-ahead optimization, when all node voltages are within [0.97, 1.03] p.u, therefore persistent jumping between the two modes can be avoided.

In a MV distribution network, r/x ratios are relatively large comparing to small ratios in high voltage transmission networks. Voltage in a distribution network is sensitive to not only reactive power but also real power. Therefore this paper proposes to use both reactive and real power to regulate voltages. In order to obtain the sensitivities a node voltage to the active and reactive power of VSC2, the hybrid AC/DC distribution network is decoupled by VSC2 into AC and DC parts since the power of the converter can be controlled actively to follow reference values. Thus the sensitivity method is applied to the AC and DC parts individually, which is not achievable for a closed-loop AC network. The sensitivities between a node voltage and the power adjustment of VSC2, Sen_P and Sen_Q , are obtained as:

$$Sen_P = \frac{\partial V_i}{\partial P_{VSC2}^{AC}} = -\frac{r_{i,VSC2}}{V_N} \quad (18)$$

$$Sen_Q = \frac{\partial V_i}{\partial Q_{VSC2}^{AC}} = -\frac{x_{i,VSC2}}{V_N} \quad (19)$$

where V_N is rated voltage, $r_{i,VSC2}$ and $x_{i,VSC2}$ are the resistance and reactance between node i and VSC2. Sen_Q is only applied for the AC side.

Thus, the real and reactive power adjustment of VSC2 can be achieved as:

$$[\Delta P] = [\Delta V]/[Sen_P] \quad (20)$$

$$[\Delta Q] = [\Delta V]/[Sen_Q] \quad (21)$$

where $[\Delta V]$ is the deviation between the measured voltage and a lower or an upper limit, which is 0.97 p.u for the under-voltage or 1.03 p.u for the over-voltage cases respectively. These adjustments affect all node voltages which are represented in equation (22).

$$\begin{bmatrix} \Delta V_1 \\ \vdots \\ \Delta V_m \\ \Delta V_{m+1} \\ \vdots \\ \Delta V_n \end{bmatrix} = \begin{bmatrix} Sen_P^1 \\ \vdots \\ Sen_P^m \\ Sen_P^{m+1} \\ \vdots \\ Sen_P^n \end{bmatrix} \cdot [\Delta P_m] + \begin{bmatrix} 0 \\ \vdots \\ 0 \\ Sen_Q^{m+1} \\ \vdots \\ Sen_Q^n \end{bmatrix} \cdot [\Delta Q_{m+1}] \quad (22)$$

where ΔP_m is power adjustment of VSC2 at the DC side, which is equal to the real power adjustment of VSC at the AC side ΔP_{m+1} ; ΔQ_{m+1} is the reactive power adjustment of VSC2 at the AC side.

If an AC node voltage is higher than 1.05p.u or lower than 0.95p.u, the reactive power of VSC2 is firstly considered to regulate the voltage because reactive power is more effective for AC voltage regulation and the DC line is not affected by the reactive power regulation of the AC side. Equation (20) is used to preliminarily calculate the adjustment of reactive power ΔQ based on the maximum voltage deviation of the measured nodes in $[\Delta V]$.

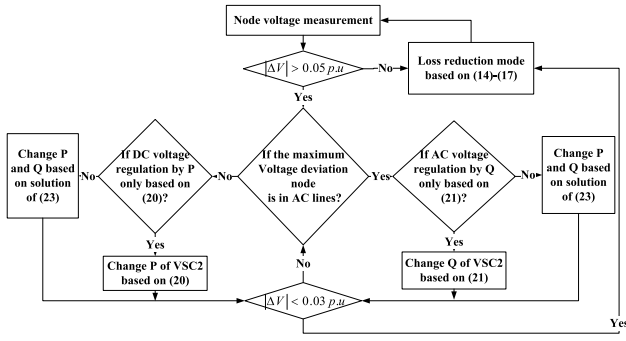


Fig. 5. Flowchart of the proposed optimization strategy.

If the reactive power adjustment ΔQ cannot be achieved due to the power rating limit of VSC2, both active and reactive power will be used to regulate node voltages.

The real and reactive power adjustment of VSC2, ΔP and ΔQ , are obtained by solving (23).

$$\begin{cases} Sen_P \cdot \Delta P + Sen_Q \cdot \Delta Q = \Delta V \\ (P_{VSC2}^{AC} + \Delta P)^2 + (Q_{VSC2}^{AC} + \Delta Q)^2 = S_{max}^{VSC2} \end{cases} \quad (23)$$

where ΔV is the maximum voltage deviation of the measured nodes. Sen_P and Sen_Q are the corresponding sensitivities of the nodes.

There will be two real solutions for quadratic equations (23). The smaller solution of ΔP is chosen for VSC2 in voltage regulation, in order to reduce the effect on the node voltages in the DC line.

If a DC node voltage is higher than 1.05 p.u. or lower than 0.95 p.u., real power is used to regulate node voltages based on equation (20). The absolute value of VSC2 reactive power will be reduced in order to release the rating of VSC2 for real power to regulate node voltages if real power is limited by current rating of VSC2, and the ΔP and ΔQ can be calculated through equation (23).

A flowchart of the proposed optimization strategy is shown in Fig. 5.

The voltage regulation mode can be implemented continuously every short time interval, e.g., 1 s depending on the measurement and communication for node voltage signals.

IV. CASE STUDY

Case studies were conducted to demonstrate the increase of power transfer capacity and DG accommodations by using a hybrid AC/DC distribution network.

A. Simulation Conditions

A 12-node double-circuit AC distribution network is shown in Fig. 6(a). There are two feeders (Line-1 and Line-2) which are connected through a circuit-breaker (CB). The sizes of conductors are taken as Copper 7 STRD cable in the case studies. The maximum transfer capacity of the AC system is 17 MW, i.e., 8.5 MW for each of the two lines. However, this capacity hasn't been fully utilized due to the voltage limits and load/DG fluctuation. This system cannot meet further increase of load demand and DG integration. Therefore, it is proposed

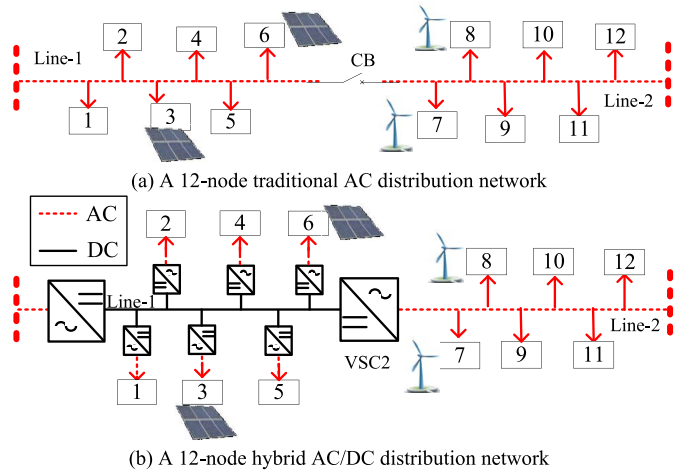


Fig. 6. Distribution networks under study.

to convert one line to DC operation to form a hybrid AC/DC distribution network shown in Fig. 6(b). The left side cables (Line-1) are converted to a symmetrical DC without neutral wire, with each 3-phase cable forming one pole. The right side cable (Line-2) remains as AC. Outputs of DGs, including wind turbines and PVs, remain as AC output. In the study, DGs are modeled as PQ node in AC-DC power flow, and the injected real power depends on available resources, while reactive power is decided by a constant power factor. Direct DC connection or DC/DC converters could be used [32] but are not considered in this study because only distribution lines are converted to DC operation, and DGs are assumed to be remained AC outputs. The AC voltage is 10 kV and the converted DC voltage is selected as $\pm 8kV$, as according to (2) $U_{DC} = 8.164kV$. The power ratings of VSC1 and VSC2 are 14 MVA and 3 MVA respectively. For comparisons, a reconfiguration method or a Back-to-back converter is also considered in the case studies. In this paper, the loss coefficients a, b, and c are set as $a = 0.011$, $b = 0.005$, $c = 0.009$ in a per unit form. As there are few existing references about the parameters in a MV distribution network, we calculate these coefficients using the method in [29] to estimate the power losses of the converters in our study.

B. Case 1 Increase of Power Transfer Capacity

Actual values of wind power, PV output and loads of a practical power system in Heilongjiang Province, China were simplified and used in case 1, as shown in Fig. 7.

In the base case with 2 AC lines without using reconfiguration, voltages of nodes 5 and 6 are lower than 0.93 p.u., and loads may have to be shed at 7 o'clock, as shown in Fig. 8(a), because loads in Line-1 are heavy while loads in Line-2 are light.

With the reconfiguration in which loads at node 6 are supplied through Line-2, voltages of all nodes are within the requirement of 0.93 p.u.–1.07 p.u. However, the reconfiguration method cannot be used too frequently due to the limited switching number a day. In addition, large transient currents maybe caused during reconfiguration, as shown in Fig. 9. The

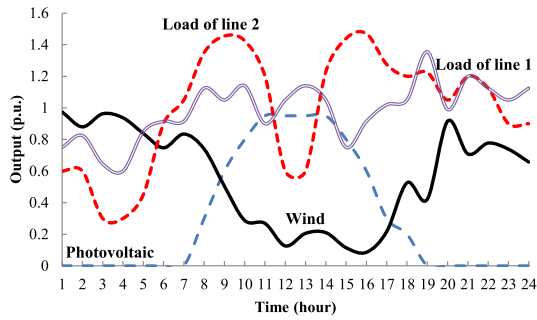


Fig. 7. One Day Load and DG Profile for case 1.

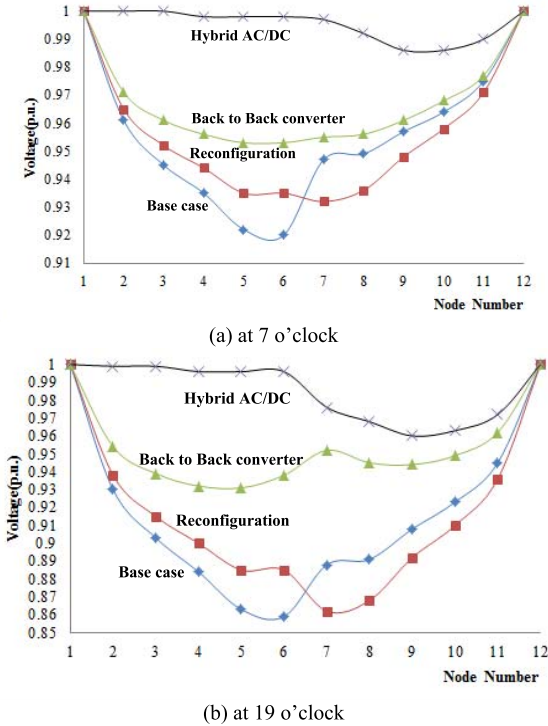


Fig. 8. Two snapshots of voltage profiles of the network.

peak current between nodes 6 and 7 is about 0.43 kA, which is 1.34 times of normal current, as shown in Fig. 9(a). The peak current of Line-1 before the node 1 reaches 0.71 kA, as shown in Fig. 9(b), which may result in a mis-trip of circuit breakers.

Due to the fast control ability of voltage source converters, VSC2 can achieve very smooth current control during power rescheduling.

Node voltages don't meet voltage requirement at 19 o'clock in the Base case and Reconfiguration case, as shown in Fig. 8(b), because loads of both lines are heavy. With a back-to-back converter, the voltages of all nodes are within the security range. This is because reactive power is compensated from the converter for both lines, and the AC Line-2 has taken 1 MW of real power from Line-1 to balance the two lines by fully using the capacity of Line-2. Node voltages of the hybrid AC/DC distribution are all within a security range and better than that with back-to-back converter because the DC line

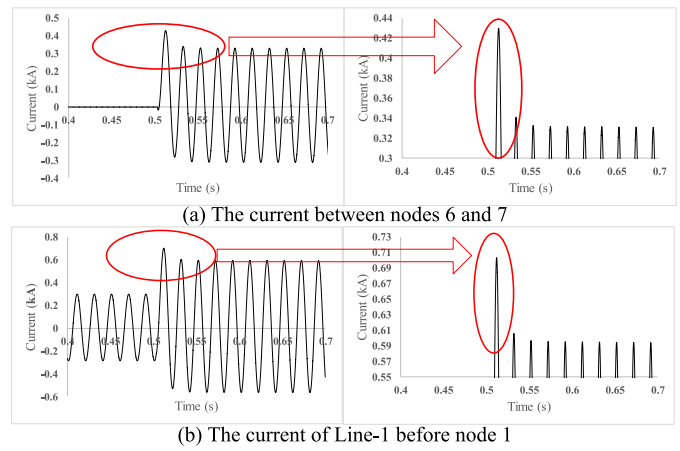


Fig. 9. Transient currents during reconfiguration.

takes over 2.23 MW of real power from the AC line, which further balance power supplying between the two lines by using the higher transfer capacity of the DC line. As shown in Fig. 8, DC side voltages are much more stable than the other loads due to the DC control of VSC1 and smaller voltage drops in DC lines.

C. Case 2 Maximum Transfer Capability

The maximum transfer capability is mainly determined by line thermal limits and node voltage limits. Assuming load power at all nodes increase at the same rate, the maximum transfer capability of the base case is about 10.5 MW when the lowest node voltage (node 6) of system reaches to 0.93 p.u., as shown in Fig. 10. This transfer capability is far below the AC line transfer capacity which is 17 MW. The maximum capability increases to about 12 MW through the network reconfiguration. The back-to-back converter can increase transfer capability to about 15 MW, when 1.07 MW of real power is injected to Line-1 from Line-2 and the remaining capacity is used to provide reactive power, i.e., 2.8 MVar is injected to both AC lines. Line-1 has reached the capacity limit and power of Line-2 has only reached 7 MW. However, reschedule more real power from Line-2 to Line-1 reduce the capacity for reactive power regulation. This will further reduce the node voltages of Line-2 below the voltage limit.

The maximum transfer capability of the AC/DC network can be increased to about 21.2 MW, which is 2.02 times of the base case, when 2.4 MW real power and 1.8 MVar reactive power are injected to the AC line (Line-2). The constraint of the maximum power transfer for the AC/DC network is the line thermal limit instead of the voltage limit, because the maximum transfer capacity of the DC line has been fully utilized without violating the voltage limit.

D. Case 3 Increase of DG Accommodation

Time domain simulation was performed to demonstrate the benefits of the proposed hybrid AC/DC distribution network on DG accommodation. Four events of DG and load variation during 10-20 s, 30-40 s, 50-60 s, and 70-80 s, as shown in Fig. 11 were used to test the control performance of VSC2.

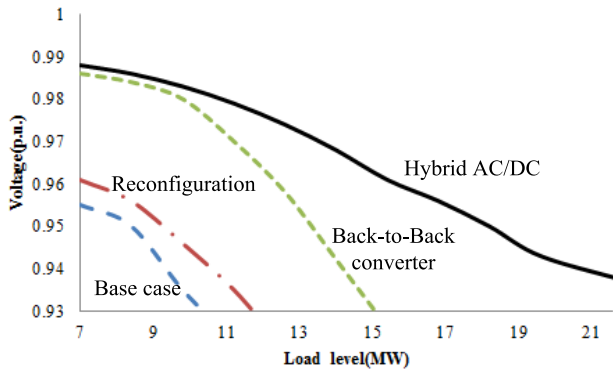


Fig. 10. The lowest node voltages under different load levels.

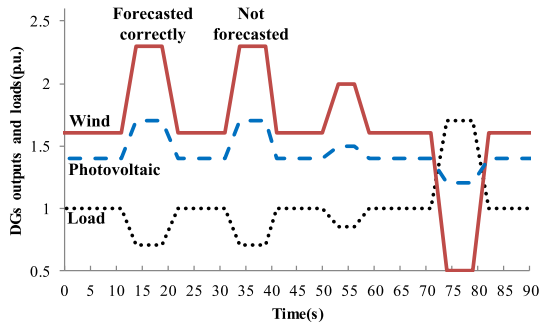


Fig. 11. Loads and DGs outputs of 90 seconds in real-time for case 2.

It is assumed that VSC2 measures node voltages and change power output every one second. This is for illustration only, as in practice a day-ahead optimization could not be achieved with such a short interval.

From 10 s to 20 s, the DG outputs and load demand reduction as shown in Fig. 11 have been forecasted correctly in advance and used for loss reduction optimization for the hybrid AC/DC network. VSC2 has thus been determined to absorb more P_{VSC2} and Q_{VSC2} from the AC side, as shown in Fig. 13, in order to maintain the voltage within the security range, as shown in Fig. 12, while in the base case or the case with the back-to-back converter, voltages have been above the risk range and violated the permitted limit.

If these DG and load variations cannot be forecasted, as shown from 30-40 s in Fig. 11, VSC2 powers do not change until the voltage of node 6 reaches 1.05 p.u at 32 s, when voltage regulation mode is triggered. According to the estimation using equation (18), from 34 s, reactive power alone cannot control the voltage back to security range. Thus, through calculation using equation (22), VSC2 reduce the real power absorbed from the AC line, in order to give more capacity for increasing reactive power absorbed from the AC line. When all the voltages are below 1.03p.u. at 37 s, VSC2 switches to the loss reduction mode, and P_{VSC2} and Q_{VSC2} come back to the initial values, This causes a slight increase in voltage again but within the security range, with a peak of 1.045 p.u at 38 s.

If the DG and load variations are small, as shown from 50-60s in Fig. 11, using only reactive power is able to control the voltage back to security range, as shown in Fig. 13.

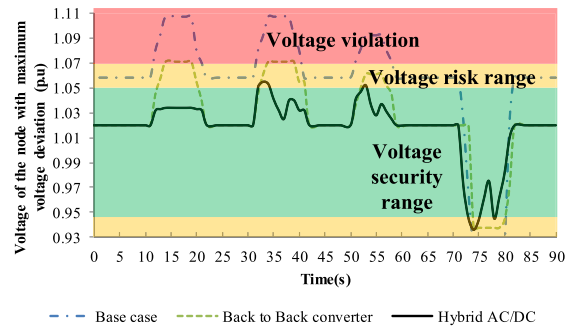


Fig. 12. Voltages deviation.

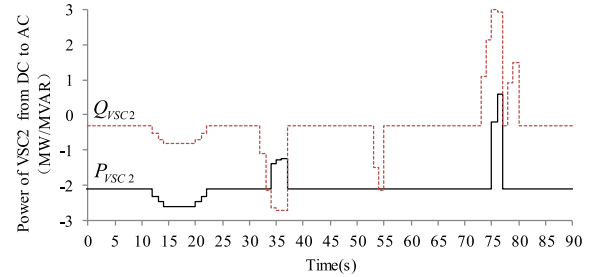


Fig. 13. Power of VSC2 from DC to AC.

If the DG outputs decrease significantly and loads increase at the same time, more reactive power needs to be injected in the AC side, while reducing the real power absorbed from the AC side can contribute to the voltage control and give more capacity space for reactive power simultaneously. The voltage regulation mode was first triggered at 73 s when the voltage is below 0.95 p.u. VSC2 switches back to the loss reduction mode at 77 s when the voltage is 0.97 p.u. This causes voltage decrease below 0.95p.u. again at 78 s. Then use of only reactive power can control the voltage above 0.97 p.u at 79 s.

E. Maximum DG Penetration

Static load flow calculation has been performed when the DG outputs increase at the same rate. The maximum DG capacity is 8.4 MW in the base case, which is about 120% of system rating, as shown in Fig. 14, when the highest node voltage (node 7) is 1.07p.u. The back-to-back converter can increase maximum DG penetration to about 160%, when 2.89 MVar of reactive power are injected to both AC lines, and 0.8 MW of real power is injected to Line-1 from Line-2. The maximum DG penetration of the hybrid AC/DC distribution network is about 200%, which is 1.67 times of the base case, and 1.25 times of the back-to-back converter, when 2.5 MW of real power and 1.6 MVar of reactive power are injected into the AC line (Line-2).

F. Discussions

The benefits and costs for building and running a hybrid AC/DC network are summarized in Table II. These are also compared with other AC cases. The benefits of a hybrid AC/DC network include reduced power losses, increased line capacity, increased utilization of line capacity, increased load

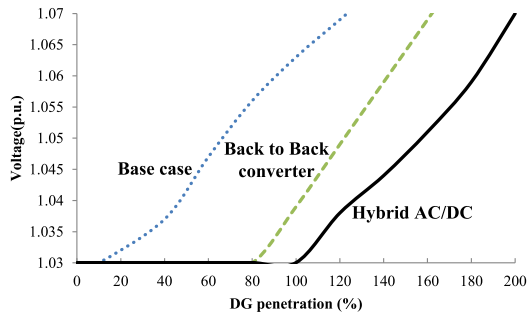


Fig. 14. The highest node voltages under different DG penetrations.

supply and DG integration, increased power quality due to VSC control, and deferring or removing the need of building new lines. The main costs are for VSC and running/monitoring DC circuits. The values for line capacities, transfer capabilities, power losses, DG accommodation, and cost of the VSCs are also given in the table.

For the circuits used in the case study, the power losses are 2907 kWh per day of the AC/DC network for load demands with a peak load of 21.2 MW. To supply the same load using AC circuits with new AC lines, the power losses would be 9912 kWh per day. Thus it is estimated that ¥1.28 M RMB would be saved in one year due to the loss reduction, assuming an electricity price of RMB ¥ 0.5/ kWh.

The maximum line capacity is increased by about 24.7% (from 17 MW to 21.2 MW) through the proposed hybrid AC/DC network, while the maximum transfer capability is increased by 102% (from 10.5 MW to 21.2 MW). This means more electricity worth ¥43 M can be served in a year. Assuming the profit rate of electricity supply is approximately 23%, the profit from the increased electricity supply is ¥10M.

The capability of DG accommodation is increased by 5.6 MW (from 8.4 MW to 14 MW) in the case study of this paper. This means that more DG integration worth ¥12 M can be achieved a year.

By converting existing AC lines to DC, huge amount of costs can be reduced by removing or deferring the need of building new AC lines. Most importantly, building a new line would be impossible in some urban areas due to very limited spaces. In addition, building a new AC line can only increase system capacity which might not be fully used due to the lack of flexible control. With VSC control, power quality including voltage and harmonic performance can be improved.

The main investments of the proposed method are the costs of converters for connecting DC links to main power supply and AC links, and connecting AC loads to the DC link.

For the circuits used in the case study, the investment of the converters is

$$\begin{aligned} & \text{¥}2\text{M/MVA} \times (14\text{MVA} + 3\text{MVA}) \\ & + \text{¥}1000/\text{kVA} \times 14000\text{kVA} = \text{¥}48\text{M} \end{aligned} \quad (24)$$

assuming that the price of VSC1 and VSC2 is ¥2 M/MVA, and the price of converters for connecting loads is 102 €/kVA [33], roughly equivalent to ¥1000/kVA. The capacities of VSC1, VSC2, and converters for connecting AC loads from DC link are 14 MVA, 3 MVA, and 14000 kVA, respectively.

TABLE II
COST BENEFITS

Cases	AC base case	AC with reconfiguration	AC with Back-to-Back converter	Hybrid AC/DC distribution network
Line capacity	Low (17 MW)	Low (17 MW)	Low (17 MW)	High (21.2 MW)
Power transfer capability	Low (10.5 MW)	Low (12 MW)	Medium (15 MW)	High (21.2 MW)
Power losses under the load of 10.5 MW	High (4911 kWh/day)	High (4013 kWh/day)	Low (1735 kWh/day)	Low (1733 kWh/day)
DG accommodation	Low (8.4 MW)	Low (8.4 MW)	Medium (11.2 MW)	High (14 MW)
Requirement of new lines	High	High	Low	Lowest
Power quality	Low	Low	High	High
VSC cost	N/A	N/A	Low (¥ 12 M)	High (¥ 48 M)
DC line operation and monitoring cost	N/A	N/A	Low	High

The investment of building new AC underground cables in urban area can be roughly estimated as:

$$\text{¥}5\text{M}/\text{km} \times 12\text{km} \times 2 = \text{¥}120\text{M} \quad (25)$$

assuming that the cost for the underground cable is ¥5 M/km [34], the line distance is 12 km, and 2 represents double circuits.

Therefore, the investment of hybrid AC/DC distribution network is much lower than that of building new AC lines. The discounted payback period is 4.96 year considering 5% discount rate according to reference [35], from the economic profits of loss reduction and increased electricity supply. If only considering the investment to the converters and profits from the electricity supply, the payback time is 4.8 year (=48/10).

These are only indicative estimation. Investments are affected by the type of loads and DGs, capacities of VSCs, costs of building spaces, voltage level, line distance, etc. Detailed analysis and comparisons should be made to select AC or DC operation. Recommendations should be made case by case.

V. CONCLUSION

This paper proposes to convert some of existing MV AC lines to DC lines and form hybrid AC/DC MV distribution networks. The increase of transfer capacities of DC circuits with different configurations converted from AC lines are analyzed and quantified. Contributions include the methods to fully achieve the maximum transfer capacity, the sensitivity method considering high *r/x* ratios and closed-loop topologies for hybrid AC/DC MV distribution networks, and the coordinated control method including not only reactive power optimization but also real power optimization.

Through the conversion, the maximum transfer capacity can be increased by 83.2% if using a symmetrical configuration with an extra conductor for single circuit cables, and by 58.7% for double circuit cables.

A VSC connecting the AC and DC lines is used to achieve flexible power scheduling and power balance, and thus to make full use of the power transfer capacity of a distribution network. A hybrid AC/DC distribution network has better performance than reconfiguring AC networks because transient currents can be avoided. AC transfer capability is constrained by voltage limits. A hybrid AC/DC distribution network can increase the capability through active and reactive power regulation.

An optimization method is designed for MV DC in urban areas. This optimization consists of the loss reduction mode and the voltage regulation mode. A day-ahead optimal dispatching is used to achieve power loss reduction and a sensitivity method considering the r/x ratio of hybrid MV distribution network is used to avoid over/under voltage caused from forecast errors. Not only reactive power optimization but also real power optimization is considered to fully achieve the maximum transfer capacity and DG accommodation.

Case studies have shown that the power transfer capability can be increased by 102% (from 10.5 MW to 21.2 MW) in a hybrid AC/DC MV distribution network, which can make full use of the capacity of DC and AC lines.

DG accommodation can be increased significantly (1.67 times in the example) using the hybrid AC/DC system under the same load level, because more power can be rescheduled flexibly between AC and DC lines through the VSC.

REFERENCES

- [1] D. Sciano *et al.*, "Evaluation of DC links on dense-load urban distribution networks," *IEEE Trans. Power Del.*, vol. 31, no. 3, pp. 1317–1326, Jun. 2016.
- [2] S. K. Chaudhary, J. M. Guerrero, and R. Teodorescu, "Enhancing the capacity of the AC distribution system using DC interlinks—A step toward future DC grid," *IEEE Trans. Smart Grid*, vol. 6, no. 4, pp. 1722–1729, Jul. 2015.
- [3] F. Capitanescu, L. F. Ochoa, H. Margossian, and N. D. Hatziargyriou, "Assessing the potential of network reconfiguration to improve distributed generation hosting capacity in active distribution systems," *IEEE Trans. Power Syst.*, vol. 30, no. 1, pp. 346–356, Jan. 2015.
- [4] F. Jing, J. H. Zhang, and R. X. Liu, "Analysis of surge current due to closing loop in distribution network," in *Proc. 8th Int. Conf. Adv. Power Syst. Control Oper. Manag.*, 2009, pp. 1–5.
- [5] M. Loos, S. Werben, and J. C. Maun, "Circulating currents in closed loop structure, a new problematic in distribution networks," in *Proc. IEEE Power Energy Soc. Gen. Meeting*, San Diego, CA, USA, 2012, pp. 1–7.
- [6] J. M. Bloemink and T. C. Green, "Benefits of distribution-level power electronics for supporting distributed generation growth," *IEEE Trans. Power Del.*, vol. 28, no. 2, pp. 911–919, Apr. 2013.
- [7] H. Qin *et al.*, "Utilisation of back-to-back VSC in a distribution network with DG," in *Proc. Int. Conf. Sci. Elect. Eng.*, Eilat, Israel, 2016, pp. 1–5.
- [8] U. Straumann and C. M. Franck, "Ion-flow field calculations of AC/DC hybrid transmission lines," *IEEE Trans. Power Del.*, vol. 28, no. 1, pp. 294–302, Jan. 2013.
- [9] M. D. Prada, L. Iguialada, C. Corchero, O. Gomis-Bellmunt, and A. Sumper, "Hybrid AC-DC offshore wind power plant topology: Optimal design," *IEEE Trans. Power Syst.*, vol. 30, no. 4, pp. 1868–1876, Jul. 2015.
- [10] H. M. A. Ahmed, A. B. Eltantawy, and M. M. A. Salama, "A planning approach for the network configuration of AC–DC hybrid distribution systems," *IEEE Trans. Smart Grid*, vol. 9, no. 3, pp. 2203–2213, May 2018, doi: [10.1109/TSG.2016.2608508](https://doi.org/10.1109/TSG.2016.2608508).
- [11] A. A. Eajal, M. F. Shaaban, K. Ponnambalam, and E. F. El-Saadany, "Stochastic Centralized dispatch scheme for AC/DC hybrid smart distribution systems," *IEEE Trans. Sustain. Energy*, vol. 7, no. 3, pp. 1046–1059, Jul. 2016.
- [12] J. Yu *et al.*, "Initial designs for the ANGLE DC project; converting existing AC cable and overhead line into DC operation," in *Proc. 13th IET Int. Conf. AC DC Power Transm.*, Manchester, U.K., 2017, pp. 1–6.
- [13] F. Nejabatkhah and Y. W. Li, "Overview of power management strategies of hybrid AC/DC microgrid," *IEEE Trans. Power Electron.*, vol. 30, no. 12, pp. 7072–7089, Dec. 2015.
- [14] T. Ma, M. H. Cintuglu, and O. Mohammed, "Control of hybrid AC/DC microgrid involving energy storage, renewable energy and pulsed loads," in *Proc. IEEE Ind. Appl. Soc. Meeting*, Addison, TX, USA, 2015, pp. 1–8.
- [15] J. Lundquist *et al.*, "Guide to the conversion of existing AC lines to DC operation," Cigré Technical Brochure 583-Working Group B2 41, 2014.
- [16] D. M. Larruskain, I. Zamora, O. Abarategui, and Z. Aginako, "Conversion of AC distribution lines into DC lines to upgrade transmission capacity," *Elect. Power Syst. Res.*, vol. 81, no. 7, pp. 1341–1348, Mar. 2011.
- [17] D. M. Larruskain, I. Zamora, O. Abarategui, and A. Iturregi, "VSC-HVDC configurations for converting AC distribution lines into DC lines," *Int. J. Elect. Power Energy Syst.*, vol. 54, no. 1, pp. 589–597, 2013.
- [18] L. Russo, G. Morana, M. Ceraolo, and P. Pelacchi, "Distribution power quality improvements using DC links with battery storage in existing networks," in *Proc. 14th Int. Conf. Exhibit. Electricity Distrib. Contributions (CIRED)*, Birmingham, U.K., 1997, pp. 1–5.
- [19] Y. Liu, X. Cao, and M. Fu, "The Upgrading renovation of an existing XLPE cable circuit by conversion of AC line to DC operation," *IEEE Trans. Power Del.*, vol. 32, no. 3, pp. 1321–1328, Jun. 2017.
- [20] K. H. Youssef, "A new method for online sensitivity-based distributed voltage control and short circuit analysis of unbalanced distribution feeders," *IEEE Trans. Smart Grid*, vol. 6, no. 3, pp. 1253–1260, May 2015.
- [21] M. Brenna *et al.*, "Automatic distributed voltage control algorithm in smart grids applications," *IEEE Trans. Smart Grid*, vol. 4, no. 2, pp. 877–885, Jun. 2013.
- [22] P. Wang *et al.*, "Integrating electrical energy storage into coordinated voltage control schemes for distribution networks," *IEEE Trans. Smart Grid*, vol. 5, no. 2, pp. 1018–1032, Mar. 2014.
- [23] "Upgrading and uprating of existing cable systems" Working Group, CIGRE TB 606 B1.11, Paris, France, Jan. 2015.
- [24] Angle-DC. 2015 *Electricity Network Innovation Competition, SP ENERGY NETWORKS*. Accessed: May 6, 2018. [Online]. Available: <http://www.ofgem.gov.uk/publications-and-updates/electricity-nic-submission-sp-energy-networks-angle-dc>
- [25] "Large cross-sections and composite screens design", Working Group, CIGRE TB 272 B1.03-2005, Jun. 2005.
- [26] K. Butler-Purry, "Distribution system modeling and analysis," *IEEE Power Energy Mag.*, vol. 11, no. 3, pp. 106–108, May/June 2012.
- [27] R. M. M. Mohd, S. A. H. Huzainie, and B. A. G. Ahmad, "Study of cable crimping factors affecting contact resistance of medium voltage cable ferrule and lug," in *Proc. Int. Conf. Exhibit. Electricity Distrib.*, Stockholm, Sweden, 2013, pp. 1–4.
- [28] F. H. M. Rafi, M. J. Hossain, and J. Lu, "Improved neutral current compensation with a four-leg PV smart VSI in a LV residential network," *IEEE Trans. Power Del.*, vol. 32, no. 5, pp. 2291–2302, Oct. 2017.
- [29] J. Lei, T. An, Z. Du, and Z. Yuan, "A general unified AC/DC power flow algorithm with MTDC," *IEEE Trans. Power Syst.*, vol. 32, no. 4, pp. 2837–2846, Jul. 2016.
- [30] H. Liang *et al.*, "Study of power flow algorithm of AC/DC distribution system including VSC-MTDC," *Energies*, vol. 8, no. 8, pp. 8391–8405, Aug. 2015.
- [31] J. Beerten, S. Cole, and R. Belmans, "Generalized steady-state VSC MTDC model for sequential AC/DC power flow algorithms," *IEEE Trans. Power Syst.*, vol. 27, no. 2, pp. 821–829, May 2012.
- [32] M. Tabari and A. Yazdani, "Stability of a dc distribution system for power system integration of plug-in hybrid electric vehicles," *IEEE Trans. Smart Grid*, vol. 5, no. 5, pp. 2564–2573, Sep. 2014.
- [33] *Voltage Source Converter (VSC) HVDC for Power Transmission-Economic Aspects and Comparison With Other AC and DC Technologies*, CIGRE Brochure, 492 WG B4.46, 2012.
- [34] *e-HIGHWAY 2050, Modular Development Plan of the Pan-European Transmission System 2050*. Accessed: May 6, 2018. [Online]. Available: http://www.e-highway2050.eu/fileadmin/documents/Results/D3_1_Technology_assessment_from_2030_to_2050.pdf
- [35] J. Sardi, N. Mithulananthan, and D. Q. Hung, "A comprehensive community energy storage planning strategy based on a cost-benefit analysis," in *Proc. Aust. Univ. Power Eng. Conf.*, Brisbane, QLD, Australia, 2016, pp. 1–6.



Lu Zhang (S'13–M'17) was born in Beijing, China in 1990. He received the B.S. degree in electrical engineering and the Ph.D. degree in agricultural electrification and automation from China Agricultural University, Beijing, in 2011 and 2016, respectively.

He is currently a Post-Doctoral Fellow with Tsinghua University. His main research interests include hybrid ac/dc distribution network, renewable energy generation, and active distribution networks.



Gen Li received the B.Eng. degree from Northeast Dianli University, Jilin, China, in 2011 and the M.Sc. degree from Nanyang Technological University, Singapore, in 2013.

He is currently recruited as a Marie Curie Early Stage Researcher and is currently pursuing the Ph.D. degree with the School of Engineering, Cardiff University, U.K. funded by the European Union's MEDOW project. His research interests include high voltage and medium voltage dc grids, power electronics, renewable power generation, and power system stability control.



Jun Liang (M'02–SM'12) received the B.S. degree from the Huazhong University of Science and Technology, Wuhan, China, in 1992, and the M.S. and Ph.D. degrees from the China Electric Power Research Institute (CEPRI), Beijing, in 1995 and 1998, respectively.

From 1998 to 2001, he was a Senior Engineer with CEPRI. From 2001 to 2005, he was with Imperial College London, U.K. as a Research Associate. From 2005 to 2007, he was with the University of Glamorgan as a Senior Lecturer. He is currently

a Professor with the School of Engineering, Cardiff University, Cardiff, U.K. He was appointed as an Adjunct Professors with the Changsha University of Science and Technology of China and North China Electric Power University, in 2014 and 2015. His research interests include HVDC, flexible ac transmission systems, power system stability control, power electronics, and renewable power generation. He is an Editorial Board Member of CSEE JPES.



Yongxiang Cai was born in Guizhou, China, in 1991. He received the B.S. degree in electrical engineering from China Agricultural University, Beijing, China, in 2014.

He is currently pursuing the Ph.D. degree with the College of Information and Electrical Engineering, China Agricultural University.



Wei Tang (M'13) received the B.Sc. degree from the Huazhong University of Science and Technology, Wuhan, China, in 1992 and the Ph.D. degree from the Harbin Institute of Technology, Harbin, China, in 1998.

From 1998 to 2000, she was a Post-Doctoral Fellow with Harbin Engineering University. She is currently a Professor with the College of Information and Electrical Engineering, China Agricultural University, Beijing, China. Her research interests include distribution network economic and security

operation, distributed generation, and active distribution network.



Wanxing Sheng (SM'13) received the B.Sc., M.Sc., and Ph.D. degrees in mechanical engineering from Xi'an Jiao tong University, Xi'an, China, in 1989, 1992, and 1995, respectively.

Since 1997, he has been a Full Professor with the China Electric Power Research Institute, Beijing, China, where he is currently the Head of the Department of Power Distribution. He is also a Leader of intelligent distribution system and an excellent expert of the State Grid Corporation of China, Beijing. He has published over 150 refereed journal and conference papers, and 15 books. His current research interests include power system analysis, renewable energy generation, and grid-connected technologies.